DOI:10.16146/j.cnki.rndlgc.2014.03.017

文章编号: 1001-2060(2014)03-0303-06

大型CFB锅炉受热面热力匹配特性研究

吴海波[1],张 缨[2],王 俊[1],廖海燕[1]
(1. 神华国华(北京)电力研究院有限公司,北京 100025; 2. 清华大学 热能工程系,北京 100049)

摘 要: 针对3台CFB锅炉的热力匹配,研究了300 MW亚临界CFB锅炉两种不同受热面布置方式下工质侧与烟气侧的热力匹配以及350 MW超临界CFB锅炉的热力匹配,定量的分析了蒸汽参数的变化对于锅炉各级受热面吸热分配的影响规律。对于超临界350 MW CFB锅炉,加热吸热的比例在21%左右,过热吸热的比例在61%左右,再热吸热的比例在18%左右;研究表明,蒸汽参数的变化对锅炉各级受热面之间的吸热分配有很大的影响,合理布置这些受热面是锅炉容量放大的关键。

关 键 词: 循环流化床; 大型化; 受热面; 热力匹配

中图分类号: TK229.6+6 **文献标识码**: A

引 言

随着世界电力设备制造技术水平的进步和经济发展需求,火力发电机组的容量不断提高,机组的单机容量也越来越大,尤其是循环流化床(CFB)锅炉技术近年来得到了迅速发展[1-2]。随着CFB锅炉容量的增加,为保证CFB锅炉炉膛的温度处于合理的水平,必须在热灰的循环回路布置更多的受热面[3],特别是在炉膛、旋风分离器、返料器等组成的固体燃料主循环回路上。主循环回路的受热面布置是CFB锅炉设计的关键,是锅炉经济安全可靠运行的保证[4-5]。目前在商业运行的300 MW CFB锅炉中,除了水冷壁、尾部对流受热面等这些常规受热面以外,其它受热面主要有两种布置方式,一是炉内布置屏式受热面,一是在外循环回路上布置外置换热器,如图1所示。合理布置这些受热面是锅炉容量放大后的关键技术之一。下面就针对这两种主流的布置方式进行研究。

1 CFB锅炉受热面布置总体介绍

针对3台CFB锅炉的热力匹配进行研究,其中两台为300 MW亚临界CFB锅炉,一台为350 MW超临界CFB锅炉。两台亚临界锅炉分别为带外置换热器(简称SUB-E锅炉)和无外置换热器的锅炉(简称SUB-P锅炉),超临界锅炉为无外置换热器的锅炉(简称SUP-P锅炉)。

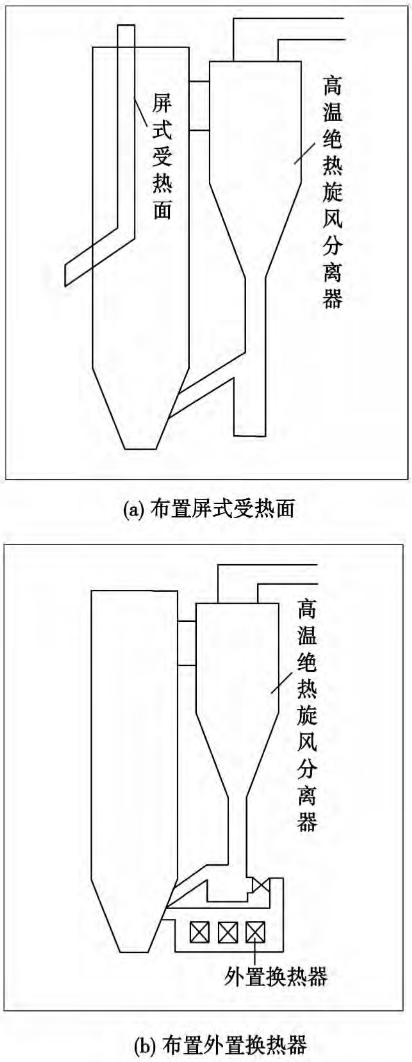

图1 CFB锅炉循环回路上受热面的不同布置方式

Fig. 1 Various arrangement modes of the heating surfaces in the the circulation loop of a CFB boiler

收稿日期: 2013-10-17; 修订日期: 2013-11-08
作者简介: 吴海波(1986-),男,内蒙锡林浩特人,神华国华(北京)电力研究院有限公司工程师.

1.1　SUB－E 锅炉

锅炉主要由炉膛、高温绝热旋风分离器、回料阀、外置换热器、尾部对流烟道、冷渣器和回转式空气预热器等部分组成，总体布置如图 2 所示[6]。

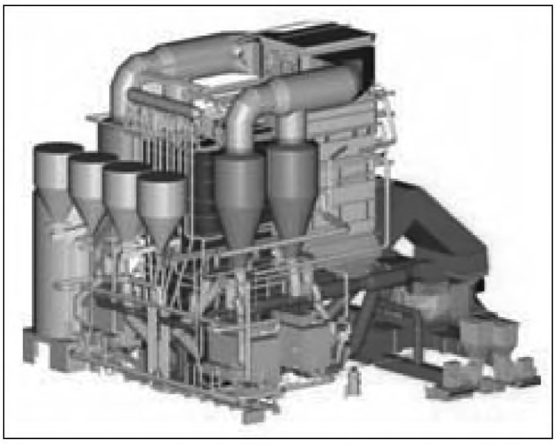

图 2　300 MW CFB 锅炉总体布置图（带外置换热器）

Fig. 2 General layout of a 300 MW CFB boiler (externally equipped with a heat exchanger)

受热面布置方式为：锅炉受热面主要在炉膛、外置换热器和尾部烟道内，炉膛内部布置水冷壁，靠近炉前的外置换热器布置高温再热器和低温过热器，靠近炉后的外置换热器布置中温过热器 I 和中温过热器 II。尾部对流烟道中依次布置高温过热器、低温再热器、省煤器和回转式空气预热器。

1.2　SUB－P 锅炉

锅炉为单筒自然循环、集中下降管、平衡通风锅炉。锅炉由一个膜式水冷壁炉膛、4 个绝热式旋风分离器、回料阀、尾部对流烟道、冷渣器和回转式空气预热器等部分组成，总体布置如图 3 所示[7]。

受热面布置方式为：受热面主要布置在炉膛与尾部烟道内，炉膛内部布置有膜式水冷壁，炉膛上部布置有水冷屏，中温过热器 I、中温过热器 II、高温屏式再热器。在尾部烟道内，设置隔墙包覆过热器，将后烟井分隔成前后两个烟道，在前烟道内布置低温再热器，在后烟道内按烟气流向依次布置低温过热器和省煤器。

1.3　SUP－P 锅炉的受热面布置方式

SUP－P 锅炉受热面的布置方式与 SUB－P 号锅炉的布置相似。受热面主要布置在炉膛与尾部烟道内，炉膛内部布置有膜式水冷壁、水冷屏、屏式中温过热器、屏式高温过热器和高温屏式再热器，尾部烟道布置有低温再热器、低温过热器和省煤器。

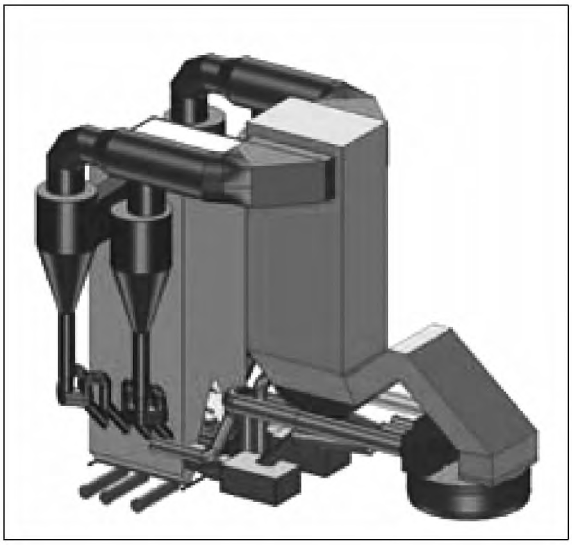

图 3　300 MW CFB 总体布置图（不带外置换热器）

Fig. 3 General layout of a 300 MW CFB boiler (externally equipped with no heat exchanger)

受热面无论是以哪种布置方式，过热汽温都通过布置在三级过热器之间的两级喷水减温器进行调节。再热汽温通过尾部烟道挡板进行调节。通过确定适当的炉膛出口温度、分析不同负荷下减温水流量以及尾部烟道挡板的开度，可以合理匹配锅炉不同受热面之间的热量。

2　各级受热面的热量分配

2.1　再热蒸汽流量的计算

可以通过调节进入外置换热器的循环物料量和调节进入尾部烟道的烟气量来调整再热蒸汽的温度，这就意味着各种负荷下的锅炉性能并非唯一确定[8]。由于再热蒸汽的压力变化很大，现场无法准确地测量出再热蒸汽量，所以根据主蒸汽量和汽轮机高压缸的抽汽量之差来间接地计算再热蒸汽量[9]。给定工况下，高温加热器（简称“高加”）的散热、泄漏以及端差的影响很小。图 4 为某电厂 300 MW 电站汽机高压缸抽汽示意图。

由 DCS 系统图可得一级抽汽压力 P_{v1}、抽汽温度 t_{v1}、二级抽汽压力 P_{v2}、抽汽温度 t_{v2}、三级抽汽压力 P_{v3}、抽汽温度 t_{v3}，进而可得一级抽汽焓 h_{v1}、二级

抽汽焓 h_{v2} 和三级抽汽焓 h_{v3}。结合各个高加的疏水温度和疏水压力，得出各级疏水焓 h_{w1}、h_{w2} 和 h_{w3}。高加的进水温度与出水温度已知，再根据从高加进口压力到高加出口压力的线性关系计算给水在高加中的压力，通过焓熵图可得各个高加进出口水的焓值 h_1、h_2、h_3 和 h_4。

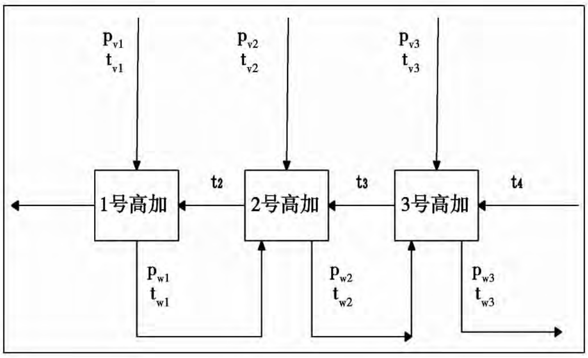

图 4　某电厂 300 MW 电站汽机高压缸抽汽示意图

Fig. 4 Schematic diagram of the steam extracted from the HP cylinder of a 300 MW steam turbine in a power plant

已知给水流量 m(t/h)，设一级抽汽量为 m_{v1}(t/h)、二级抽汽量为 m_{v2}(t/h)、三级抽汽量为 m_{v3}(t/h)。据热平衡关系有：

1 号高加热平衡：

$$m(h_1 - h_2) = m_{v1}(h_{v1} - h_{w1})$$

2 号高加热平衡：

$$m(h_2 - h_3) = m_{v2}(h_{v2} - h_{w2}) + m_{v1}(h_{w1} - h_{w2})$$

3 号高加热平衡：

$$m(h_3 - h_4) = m_{v3}(h_{v3} - h_{w3}) + (m_{v1} + m_{v2})(h_{w2} - h_{w3})$$

联立方程，可得一、二、三级抽汽量 m_{v1}，m_{v2}，m_{v3} 的值。又知不同负荷下主蒸汽流量 m_v，t/h，那么再热蒸汽流量为 $m_v - m_{v1} - m_{v2} - m_{v3}$，t/h。

通过计算，分别得到了 SUB－E 锅炉、SUB－P 锅炉和 SUP－P 锅炉的再热蒸汽流量，如表 1 所示。

表 1　再热蒸汽流量

Tab. 1 Reheat steam flow rate

电厂	SUB－P			SUB－E			SUP－P
负荷(BMCR)/%	69	82	94	71	83	96	100
再热蒸汽流量/t·h^{-1}	582	687	854	498	631	766	991

2.2　各级受热面的热量分配计算方法

再热蒸汽流量计算得到后，根据现场数据以及减温水喷入前后的能量守恒定律，可以得到流经其他各级过热器的流量，再根据各级受热面的焓增，获得各级受热面的吸热量，进而可以得到锅炉各级受热面的热量分配。本例分别计算以上 3 台锅炉各级受热面的热量分配，以下所提“负荷”均为锅炉最大连续蒸发量负荷。

由于这几台锅炉燃料的性质差别不是很大，下面就将不同锅炉的各级受热面热力分配进行对比研究。

3　结果与讨论

3.1　SUB－E 锅炉

3.1.1　工质侧的吸热份额

图 5 为 300 MW 带外置换热器 CFB 锅炉工质侧的热力匹配。从图中可以看出，随着负荷的增大，水冷壁的吸热量减少，但减少幅度较无外置换热器的幅度小。这是由于两个因素共同作用的结果，首先，随着压力的增大，汽化潜热减小，吸热量减小，其次由于外置换热器的调节作用，带外置换热器锅炉的床温随着负荷的变化不大，在低负荷时，床温也较高，那么相对的吸热量也越大。综合这两个因素，水冷壁的吸热量份额减少幅度不大。

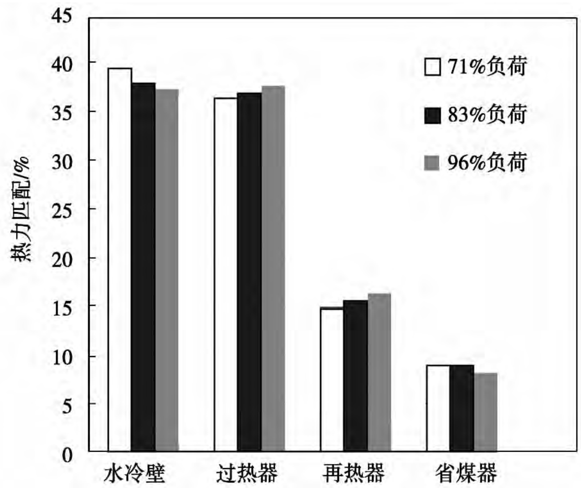

图 5　300 MW 带外置换热器受热面锅炉的热力匹配

Fig. 5 Heat matching of a 300 MW CFB boiler externally provided with a heat exchanger serving as the heating surface

过热和再热受热面布置在外置换热器内，随着负荷的增大，进入到外置换热器内的循环物料量增大，因此，过热器和再热器的吸热量随着负荷的升高而增大，但是外置换热器的传热性能好，汽温调节灵活，使得过热和再热吸热变化幅度较炉膛内布置的屏式受热面吸热变化小。

同等条件下，带外置换热器炉膛的出口烟温比无外置换热器锅炉的炉膛出口烟温略高，但是带外置换热器锅炉尾部布置了高温过热器，低温再热器、省煤器和空气预热器，而无外置换热器的锅炉尾部布置了低温过热器、低温再热器、省煤器和空气预热器，所以对于带外置换热器与无外置换热器的锅炉，省煤器的吸热份额相差不大，且对于带外置换热器的锅炉，随负荷变化省煤器的吸热份额变化不明显。

3.1.2 烟气侧的吸热份额

图6 给出了 300 MW 带外置换热器的 CFB 锅炉烟气侧热力匹配。总体来说，随着锅炉负荷的增加，外置换热器的吸热份额增大，而炉膛内的吸热份额则随之降低，尾部烟道吸热份额无显著变化。这主要是由于单位质量的工质的蒸发吸热降低，过热吸热增加。炉膛内主要布置蒸发受热面，这时单位质量的工质吸热量减少，导致吸热比例的下降，而外置式换热器内布置有过热器和再热器，过热段和再热段的吸热比例将随之增加。

图 6 中，外置换热器的吸热份额明显高于该锅炉的设计值。分析认为，由于锅炉所燃用的煤炭热值偏低，循环灰流量增大，导致外置换热器内的受热面吸热增加，减温水也相应增加。相当于外置换热器中的部分过热管束，实际上成为蒸发受热面。

3.2 SUB－P 的锅炉

3.2.1 工质侧的吸热份额

图7 为 300 MW 无外置换热器 CFB 锅炉工质侧的热力匹配。从图中可以看出，随着锅炉负荷的增加，水冷壁和省煤器的吸热量减少，过热器和再热器的吸热量增加。这是由于: 在亚临界参数的锅炉中，工质加热吸热主要靠省煤器完成，蒸发吸热主要靠水冷壁完成，而过热吸热则由过热器完成，因此随着负荷的增大，工质压力增大，水的汽化潜热减少，使得加热吸热量减少，过热吸热量增加。所以在水冷壁的蒸发吸热量减少，过热吸热和再热吸热增大。负荷的改变对于省煤器的吸热量的影响较小，但由于随着负荷的增大，省煤器进口水温是递增的，出口水温值差别不大。所以随着负荷的增大，在省煤器中的吸热量随之减少。

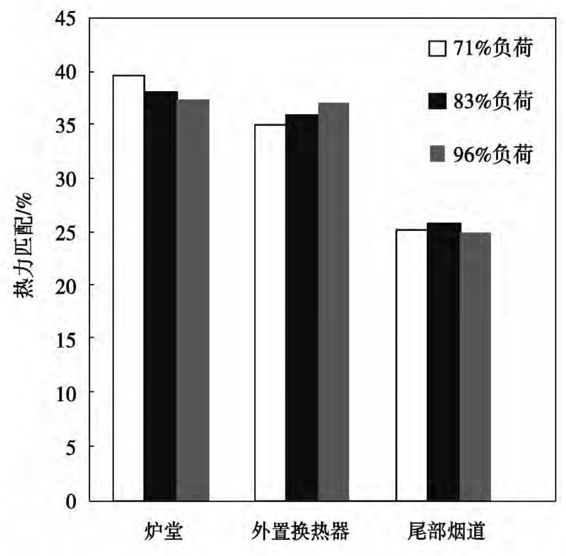

图 6 300 MW 带外置换热器受热面锅炉的热力匹配

Fig. 6 Heat matching of a 300 MW CFB boiler externally provided with a heat exchanger serving as the heating surface

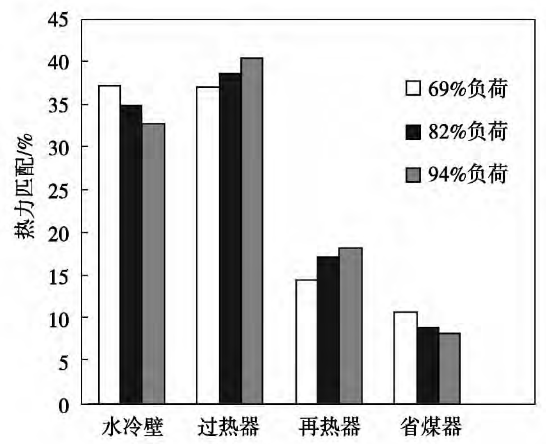

图 7 300 MW 无外置换热器锅炉的热力匹配

Fig. 7 Heat matching of a 300 MW CFB boiler externally provided with no heat exchanger serving as the heating surface

3.2.2 烟气侧的吸热份额

图8 为 300 MW 无外置换热器 CFB 锅炉烟气侧的热力匹配。从图中可以看出，锅炉 60% 以上的吸热量是在炉内完成。在较低负荷时，炉膛的吸热量

所占比例较大，这可能是由于在低负荷时，工质压力较低，使得水冷壁吸热较大，屏式受热面吸热较小，综合两因素，使得布置在炉内的屏式受热面与水冷壁的吸热总和较大，即炉膛吸热量较大。但是达到一定负荷时，随着负荷的增大，炉膛吸热与尾部吸热变化不明显。

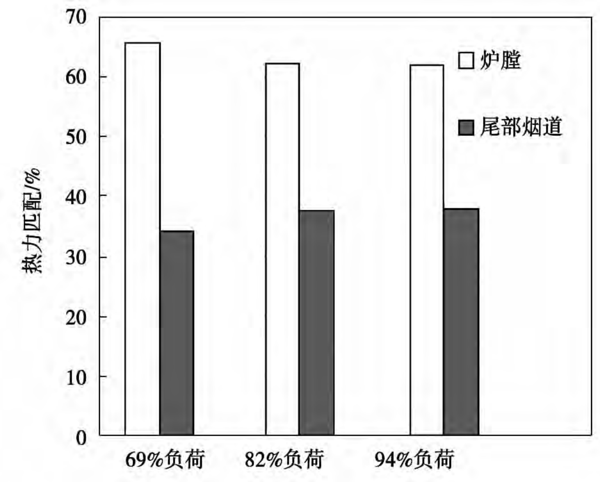

图 8　300 MW 无外置换热器锅炉的热力匹配

Fig. 8 Heat matching of a 300 MW CFB boiler externally provided with no heat exchanger serving as the heating surface

3.3　SUP－P 锅炉

图 9(a) 为超临界 350 MW CFB 锅炉在 BMCR 负荷时的热力分配，图 9(b) 为亚临界 300 MW CFB 锅炉在 94% BMCR 负荷时的热力分配。从两图对比可以看出，就工质侧的吸热而言，水冷壁的吸热份额相当，而超临界锅炉省煤器的吸热份额高于亚临界锅炉，这是由于对于超临界锅炉加热吸热主要在省煤器中完成，而亚临界锅炉的加热吸热在省煤器与水冷壁中共同完成，对于超临界 CFB 锅炉，工质没有蒸发吸热量，因此过热吸热份额大大增大，加热份额较小，变化幅度较亚临界锅炉相差不大。

通过确定饱和水焓、饱和蒸汽焓以及过热蒸汽临界点的蒸汽焓值，根据焓差可以得到其热力匹配。对于超临界锅炉，过热吸热是在水冷壁和过热器中完成的，从图 10 可以看出，加热吸热的比例在 21% 左右，过热吸热的比例在 61% 左右，再热吸热比例在 18% 左右。从图 11 可以看出，对于亚临界锅炉，加热吸热与再热吸热的份额与其超临界的份额差别不大，而蒸发吸热与过热吸热之和与超临界的过热吸热相当。

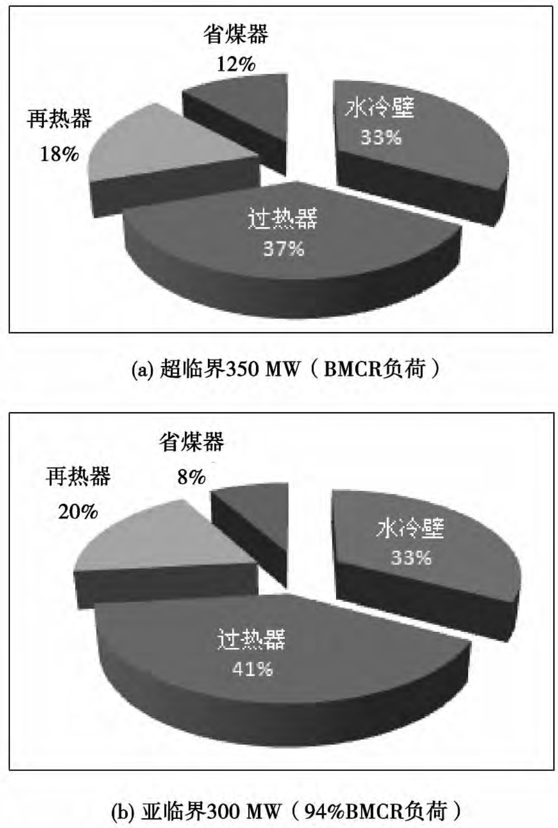

图 9　超临界 350 MW 锅炉与亚临界 300 MW 锅炉的热力分配比较

Fig. 9 Comparison between the heat matching of a 350 MW supercritical boiler and a 300 MW subcritical boiler

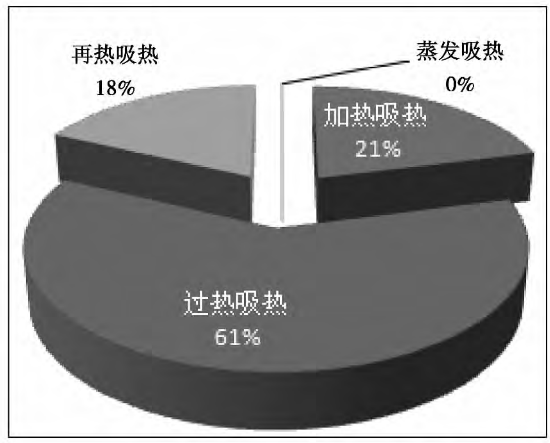

图 10　超临界 350 MW 锅炉的热力分配

Fig. 10 Heat distribution of a 350 MW supercritical boiler

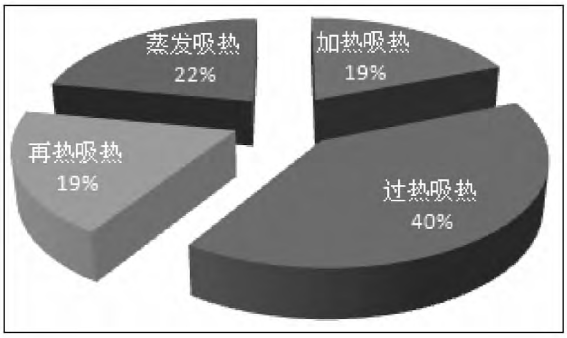

图 11　亚临界 300 MW 锅炉的热力分配
Fig. 11 Heat distribution of a 300 MW subcritical boiler

由于从亚临界锅炉到超临界锅炉的变化或锅炉负荷的改变，使得蒸汽参数的变化对于锅炉的各个受热面之间的吸热量分配有很大影响，吸热分配比例的不同，将直接影响受热面的布置、受热面类型的选择以及材料的选择等。因此，合理布置这些受热面是锅炉容量放大的关键技术之一。

4 结　论

(1) 研究了 300 MW 亚临界 CFB 锅炉两种不同受热面布置方式下工质侧与烟气侧的热力匹配以及 350 MW 超临界 CFB 锅炉的热力匹配特性，可为 CFB 锅炉设计和容量放大提供参考;

(2) 对于超临界 350 MW CFB 锅炉，加热吸热的比例在 21% 左右，过热吸热的比例在 61% 左右，再热吸热比例在 18% 左右;

(3) 蒸汽参数的变化对于锅炉各级受热面之间的吸热分配有很大影响，合理布置这些受热面是锅炉容量放大的关键技术之一。

参考文献:

[1] 李　斌，李建锋，吕俊复，等. 我国大型循环流化床锅炉机组运行现状 [J]. 锅炉技术，2012，43(1):22-27.
LI Bin，LI Jian-feng，LU Jun-fu，et al. Current status of the operation of large-sized circulating fluidized bed boiler units in China [J]. Boiler Technology，2012，43(1):22-27.

[2] 蒋敏华，孙献斌. 大型循环流化床锅炉的开发研制 [J]. 中国电机工程学报，2007，27(23):51-56.
JIANG Min-hua，SUN Xian-bin. Research and development of large-sized CFB boilers in China [J]. Proceedings of China Electric Machinery Engineering，2007，27(23):51-56.

[3] Wu Haibo，Zhang Man，Lu Qinggang，et al. The Heat Transfer Coefficients of the Heating Surface of 300 MWe CFB Boiler [J]. Journal of Thermal Science，2012，21(4): 368-376.

[4] Sundaresan R，Ajit Kumar Kolar. Core Heat Transfer Studies in a Circulating Fluidized Bed [J]. Journal of Powder Technology，2002 (124):548-554.

[5] C Breitholtz，B Leckner，A P Baskakov. Wall Average Heat Transfer in CFB Boilers [J]. Journal of Powder Technology，2001(120): 41-48.

[6] 聂　立，王鹏，霍锁善，等. 东方型 300 MW 循环流化床锅炉开发设计 [J]. 东方电气评论，2007，21(2): 18-21.
NIE Li，WANG Peng，HUO Suo-shan，et al. Development and design of a Dongfang type 300 MW CFB boiler [J]. Dongfang Electrical Review，2007，21(2): 18-21.

[7] 蒋敏华，肖　平. 大型循环流化床锅炉技术 [M]. 北京: 中国电力出版社，2009.
JIANG Min-hua，XIAO Ping. Large-sized circulating fluidized bed boiler technology [M]. Beijing: Chinese Electric Power Press，2009.

[8] 吕俊复. 超临界循环流化床锅炉水冷壁热负荷及水动力研究 [D]. 北京: 清华大学，2004.
LU Jun-fu. Heat load and hydrodynamic investigation of the water walls of a supercritical circulating fluidized bed boiler [D]. Beijing: Tsinghua University，2004.

[9] 杨　磊. 循环流化床锅炉外置式换热器热态实验研究 [D]. 重庆: 重庆大学，2007.
YANG Lei. Hot-state test research of a circulating fluidized bed boiler externally provided with a heat exchanger [D]. Chongqing: Chongqing University，2007.

(丛　敏　编辑)

& Power. – 2014,29(3). –297 –302

By using the numerical simulation method, reviewed was the influence of the root air on the air flow characteristics of a fuel oil swirling burner thus designed under the supercharging condition. By analyzing the corresponding returning flow zone distribution, velocity distribution and resistance characteristics etc. in various flow areas for the root air, the authors concluded that for the swirling burner under discussion, the influence of the root air on the supercharged air flow characteristics mainly reflects the magnitude of the air quantity passing through the root, i. e. the opening area of the combustion stabilizer and is irrelevant to the mode for drilling holes and the diameter of a single hole. Among them, the ratio of the area of the holes and the surface area of the combustion stabilizer f/F = 0.18 was regarded as the optimum parameter. The axial speed distribution on various representative sections corresponding to the various areas of the flow path for the root air all assumed a shape of "M" while the tangential speed distribution took a shape of "N". When f/F = 0, the location of the stagnation point in the central returning flow zone lagged behind by 0.17 as compared with those when f/F = 0.18 and f/F = 0.36. When f/F = 0.54, there existed no stagnation point in the central returning flow zone. The resistance loss occurred during the air flowing through the locations of the blades and the combustion stabilizer occupied a highest proportion of the total resistance loss. Both the total flow resistance and the area of the flow path for the root air assumed a monotone descending linear relationship. The relative error of the resistance coefficient between the calculated value and the test one was invariably lower than 2%, further proving that the calculation model thus chosen is rational. **Key words:** root air, returning flow zone, velocity distribution, resistance characteristics

大型 CFB 锅炉受热面热力匹配特性研究 = Study of the Thermal Matching Characteristics of the Heating Surfaces of a Large-sized CFB (Circulating Fluidized Bed) Boiler [刊,汉] WU Hai-bo, WANG Jun, LIAO Hai-yan (Shenhua Guohua (Beijing) Electric Power Research Institute Co. Ltd., Beijing, China, Post Code: 100025), ZHANG Man (Department of Engineering for Thermal Energy, Tsinghua University, Beijing, China, Post Code: 100049) //Journal of Engineering for Thermal Energy & Power. – 2014,29(3). –303 –308

In the light of the thermal matching of three boilers, studied were the thermal matching of the working medium side and the flue gas side of a 300 MWe subcritical CFB boiler in two different heating surface arrangement modes and that of a 350 MWe supercritical CFB boiler and quantitatively analyzed was the law governing the influence of changes in the steam parameters on the distribution of heat absorbed by various heating surfaces at various levels of the boilers. For a 350 MW CFB boiler, the proportion of heat absorbed during the evaporation process of feedwater is around 21%, that during the superheating process about 61% and that during the reheating process approximately 18%. It has been found that changes in steam parameters have a very big influence on the distribution of heat absorbed by various heating surfaces at various levels, thus proper arrangement of these heating surfaces becomes the

key to the capacity expansion of the boiler. **Key words:** circulating fluidized bed, large-sized orientation, heating surface, thermal matching

蒸汽疏水阀门内漏量定量诊断方法研究 = Study of the Methods for Quantitatively Diagnosing the Inner Leakage Flow Rate of a Steam Trap [刊,汉] LIU Yang, LI Lu-ping, LIU Gong-chun, HUANG Zhang-jun (College of Energy Source and Power Engineering, Changsha University of Science and Technology, Changsha, China, Post Code: 410014), KONG Hua-shan, DENG You-cheng (Hunan Hongyuan High Pressure Valve Co. Ltd., Zhuzhou, China, Post Code: 412100) //Journal of Engineering for Thermal Energy & Power. -2014, 29(3). -309 -314

Through a simulation calculation of the leakage flow rate of a valve, the authors obtained the variation law governing the changes of the tube wall temperature characteristic parameter of the drainage pipeline before the valve with the parameters of the working medium leaked, leakage flow rate, inner diameter of the tubes, tube wall thickness, insulation layer thickness and ambient temperature. Calculated by using a linear regression model, the authors also obtained a quantitative correlation formula between the tube wall temperature and the leakage flow rate at the point under discussion. In combination with the quantitative correlation formula, the authors also formulated a standard for quantitatively diagnosing the inner leakage flow rate of a valve and checked by using the test data published by the literature. The test results show that the correlation formula has sufficient accuracy and can be used for diagnosing any inner leakage fault of a steam trap. **Key words:** leakage flow rate, tube wall temperature, least square method, quantitative correlation formula

FLUENT **中煤粉燃烧飞灰含碳量数值模型的改进 = Improvement of the Numerical Model for Determining the Carbon Content of Flying Ash During Combustion of Pulverized Coal Contained in the Software Fluent [刊,汉]** CHEN Shi-he, ZHU Ya-qing, LUO Jia (Guangdong Power Grid Corporation, Academy of Electric Power Sciences, Guangzhou, China, Post Code: 510080), JI Jun-jie (Shanghai Kaili Research and Development Center, Shanghai, China, Post Code: 201206) //Journal of Engineering for Thermal Energy & Power. -2014, 29(3). -315 -319

To enhance the precision predicting the carbon content of flying ash from a pulverized coal-fired boiler in a power plant by using the software Fluent, deducted was the core shrinkage model for coke with the dispersion resistance in the ash layer being taken into account and improved was the coke combustion model contained in the software Fluent by itself based on the "multiple surface reaction" framework provided by the software Fluent and in combination with the user defined function technology. On this basis, the self-contained and improved combustion model for coke